
Fast Certified Robust Training with Short Warmup

Zhouxing Shi^{1*}, Yihan Wang^{1*}, Huan Zhang^{1,2}, Jinfeng Yi³, Cho-Jui Hsieh¹

¹UCLA ²CMU ³JD AI Research

zshi@cs.ucla.edu, yihanwang@cs.ucla.edu, huan@huan-zhang.com,

yijinfeng@jd.com, chohsieh@cs.ucla.edu

* Equal contribution

Abstract

Recently, bound propagation based certified robust training methods have been proposed for training neural networks with certifiable robustness guarantees. Despite that state-of-the-art (SOTA) methods including interval bound propagation (IBP) and CROWN-IBP have per-batch training complexity similar to standard neural network training, they usually use a long warmup schedule with hundreds or thousands epochs to reach SOTA performance and are thus still costly. In this paper, we identify two important issues in existing methods, namely exploded bounds at initialization, and the imbalance in ReLU activation states and improve IBP training. These two issues make certified training difficult and unstable, and thereby long warmup schedules were needed in prior works. To mitigate these issues and conduct faster certified training with shorter warmup, we propose three improvements based on IBP training: 1) We derive a new weight initialization method for IBP training; 2) We propose to fully add Batch Normalization (BN) to each layer in the model, since we find BN can reduce the imbalance in ReLU activation states; 3) We also design regularization to explicitly tighten certified bounds and balance ReLU activation states during warmup. We are able to obtain **65.03%** verified error on CIFAR-10 ($\epsilon = \frac{8}{255}$) and **82.36%** verified error on Tiny-ImageNet ($\epsilon = \frac{1}{255}$) using very short training schedules (**160 and 80 total epochs**, respectively), outperforming literature SOTA trained with hundreds or thousands epochs under the same network architecture. The code is available at <https://github.com/shizhouxing/Fast-Certified-Robust-Training>.

1 Introduction

While deep neural networks (DNNs) are successfully applied in various areas, its robustness problem has attracted great attention since the discovery of adversarial examples (Szegedy et al., 2013; Goodfellow et al., 2015; Carlini & Wagner, 2017; Kurakin et al., 2016; Chen et al., 2017; Madry et al., 2018; Su et al., 2018; Choi et al., 2019), which poses concerns in DNN applications especially the safety-critical ones such as autonomous driving. Methods for improving the empirical robustness of DNNs, such as adversarial training (Madry et al., 2018), provide no provable robustness guarantees, and thus some recent works aim to pursue *certified robustness*. Specifically, the robustness is evaluated in a certifiable manner using robustness verifiers (Katz et al., 2017; Zhang et al., 2018; Wong & Kolter, 2018; Singh et al., 2018, 2019; Bunel et al., 2017; Raghunathan et al., 2018b; Wang et al., 2018b; Xu et al., 2020; Wang et al., 2021), which verify whether the model is provably robust against all possible input perturbations within the range. This is achieved usually by efficiently computing the output bounds.

To improve certified robustness, *certified robust training* methods (also referred to as certified defense) minimize a certified robust loss computed by a verifier, and the certified loss is an upper bound of the worst-case loss given specified input perturbations. So far, Interval Bound Propagation (IBP) (Gowal

et al., 2018; Mirman et al., 2018) and CROWN-IBP (Zhang et al., 2020; Xu et al., 2020) are the most efficient and effective methods for general models. IBP computes an interval with the output lower and upper bounds for each neuron, and CROWN-IBP further combines IBP with tighter linear relaxation-based bounds (Zhang et al., 2018; Singh et al., 2019) during warmup.

Both IBP and CROWN-IBP with loss fusion (Xu et al., 2020) have a per-batch training time complexity similar to standard DNN training. However, certified robust training remains costly and challenging, mainly due to their unstable training behavior – they could easily diverge or stuck at a degenerate solution without a long “warmup” schedule. The warmup schedule here refers to training the model with a regular (non-robust) loss first and then gradually increasing the perturbation radius from 0 to the target value in the robust loss (some previous works also refer to it as “ramp-up”). For example, generalized CROWN-IBP in Xu et al. (2020) used 900 epochs for warmup and 2,000 epochs in total to train a convolutional model on CIFAR-10 (Krizhevsky et al., 2009).

In this paper, we identify two important issues in existing certified training, so that a long warmup schedule could not be easily removed in previous works. First, we find that the certified bounds can explode at the start of training, which is partly due to the suboptimal *weight initialization* in prior works. A good weight initialization is important for successful DNN training (Glorot & Bengio, 2010; He et al., 2015a), but prior works for certified training generally use weight initialization methods originally designed for standard DNN training, while certified training is essentially optimizing a different type of augmented network defined by robustness verification (Zhang et al., 2020). The long warmup with gradually increasing perturbation radii in prior works can somewhat be viewed as finding a better initialization for final IBP training with the target radius, but it is too costly. Second, we also observe that *IBP leads to imbalanced ReLU activation states*, where the model prefers inactive (dead) ReLU neurons significantly more than other states because inactive neurons tend to tighten IBP bounds. It can however hamper classification performance if too many neurons are dead. This issue can become more severe if the warmup schedule is shorter.

We focus on improving IBP training, since IBP is efficient per batch, and it is also the base of recent state-of-the-art methods (Zhang et al., 2020; Xu et al., 2020). We propose the following improvements:

- We derive a new weight initialization, *IBP initialization*, for IBP-based certified training. The new initialization can stabilize the tightness of certified bounds at initialization.
- We identify the benefit of Batch Normalization (BN) in certified training, and we find BN which normalizes pre-activation outputs can balance ReLU activation states and also stabilize variance. We propose to fully add BN to every layer, while it was partly or fully missed in prior works.
- We further propose regularizers to explicitly stabilize certified bounds and balance ReLU activation states during warmup.

We are able to efficiently train certifiably robust models that outperform previous SOTA performance in significantly shorter training epochs. We achieve a verified error of **65.03%** ($\epsilon = \frac{8}{255}$) on CIFAR-10 in **160** total training epochs, and **82.36%** on TinyImageNet ($\epsilon = \frac{1}{255}$) in **80** epochs, based on efficient IBP training. Under the same convolution-based architecture, we significantly reduce the total training cost by 20 ~ 60 times compared to previous SOTA (Zhang et al., 2020; Xu et al., 2020) or concurrent work (Lyu et al., 2021).

2 Background and Related Work

2.1 Certified Robust Training

Training robust neural networks can generally be viewed as solving the following min-max optimization problem:

$$\min_{\theta} \mathbb{E}_{(\mathbf{x}, y) \in \mathcal{X}} \left[\max_{\delta \in \Delta(\mathbf{x})} L(f_{\theta}(\mathbf{x} + \delta), y) \right], \quad (1)$$

where f_{θ} stands for a neural network parameterized by θ , \mathcal{X} is the data distribution, \mathbf{x} is a data example, y is its ground-truth label, δ is a perturbation constrained by specification $\Delta(\mathbf{x})$, and L is the loss function. Empirical *adversarial training* methods (Goodfellow et al., 2015; Madry et al., 2018) solve the inner maximization in Eq. (1) with adversarial attack, and then solve the outer

minimization as regular DNN training but augmented with δ . However, in adversarial training, the inner maximization has no guarantee to find a δ which can lead to worst model performance. In contrast, *certified robust training* methods compute a certified upper bound for the inner maximization, so that the upper bound provably covers the worst-case perturbation.

In terms of certified robustness works, Raghunathan et al. (2018a) used semidefinite relaxations for small two-layer models, and Wong & Kolter (2018); Mirman et al. (2018); Dvijotham et al. (2018); Wang et al. (2018a) used linear relaxations but are still too computationally expensive for large models. On the other hand, Mirman et al. (2018) first used interval bounds to train a certifiably robust network, and Gowal et al. (2018) made it more effective. This approach is often referred to as interval bound propagation (IBP). CROWN-IBP (Zhang et al., 2020) further combined IBP with tighter linear relaxation bounds by CROWN (Zhang et al., 2018) during warmup, and it is generalized and accelerated in Xu et al. (2020). Additionally, Balunovic & Vechev (2020) combined certified training with adversarial training; Xiao et al. (2019) added a ReLU stability regularizer to empirical adversarial training, to reduce unstable neurons for faster and tighter verification when tested with mixed integer programming (MIP), but their objective is distinct from ours and this method was shown not to improve certified training (Lee et al., 2021). In concurrent works, Lyu et al. (2021) proposed a parameterized ramp function as an alternative activation function, and used a tighter linear bound propagation algorithm for verification; Zhang et al. (2021) proposed to use a different architecture with “ ℓ_∞ -distance neurons” instead of traditional linear or convolutional layers. Yet they still need long training schedules.

Moreover, while our scope in this paper is deterministic certified robustness, there are also randomization based works for probabilistic certified defense (Cohen et al., 2019; Li et al., 2019; Lecuyer et al., 2019; Salman et al., 2019). But randomized smoothing requires costly sampling at test time, and it is usually for ℓ_2 perturbations and has fundamental limitations for ℓ_∞ ones (Yang et al., 2020; Blum et al., 2020; Kumar et al., 2020).

2.2 Weight Initialization of Neural Networks

Many prior works have studied the weight initialization for standard DNN training. Xavier or Glorot initialization (Glorot & Bengio, 2010), adopted by popular deep learning libraries such as PyTorch (Paszke et al., 2019) and Tensorflow (Abadi et al., 2016) as the default initialization, aim to stabilize the magnitude of forward propagation and gradient backpropagation signals measured with variance. It uses a uniform distribution or normal distribution to independently initialize each element in the weight matrix with a derived variance for the distribution. He et al. (2015a) derived an initialization that more accurately stabilizes the variance in ReLU networks. Saxe et al. (2013) proposed an orthogonal initialization which may lead to better learning dynamics. Some other works also derived initializations for specific DNN structures (Taki, 2017; Huang et al., 2020), and Bhattacharya (2020); Zhu et al. (2021) proposed to automatically learning initializations. However, these initializations were designed for standard DNN training, while they can generally lead to exploded certified bounds for IBP training as we will show in this paper.

2.3 Batch Normalization for DNN Training

Batch normalization (BN) (Ioffe & Szegedy, 2015) is originally proposed to improve DNN training by reducing interval covariate shift. More recently, Santurkar et al. (2018) instead suggests that BN actually improves DNN training by smoothing the loss landscape without the necessity of reducing internal covariate shift, and BN can accelerate DNN training (Van Laarhoven, 2017). In this paper, we identify the extra benefit of using BN in IBP training.

3 Methodology

3.1 Notations and Definitions

We focus on improving IBP training, and we consider a commonly adopted ℓ_∞ perturbation setting in adversarial robustness on a K -way classification task. For a DNN $f_\theta(\mathbf{x})$ with clean input \mathbf{x} , there can be some perturbation δ satisfying $\|\delta\|_\infty \leq \epsilon$, and the actual perturbed input to the model is $\mathbf{x} + \delta$.

In robustness verification for achieving certified robustness, we verify whether

$$[f_\theta(\mathbf{x} + \delta)]_y - [f_\theta(\mathbf{x} + \delta)]_i > 0, \quad \forall i, \delta \text{ s.t. } i \neq y, \|\delta\|_\infty \leq \epsilon, \quad (2)$$

holds true, where $[f_\theta(\mathbf{x} + \delta)]_i$ is the logits score for class i and y is the ground-truth. This is equivalent to verifying whether the DNN provably makes correct prediction for all input $\mathbf{x} + \delta$ ($\|\delta\|_\infty \leq \epsilon$). For network f_θ , we assume that there are m hidden affine layers (either convolutional or fully-connected layers) with ReLU activation. We use \mathbf{h}_i to denote the pre-activation output value of the i -th layer, and $\mathbf{h}_{i,j}$ denotes the j -th neuron in the i -th layer. We also use $\mathbf{z}_i = \text{ReLU}(\mathbf{h}_i)$ to denote the post-activation value. For a convolutional or fully-connected layer, we use \mathbf{W}_i and \mathbf{b}_i to denote its parameters, where $\mathbf{W}_i \in \mathbb{R}^{r_i \times n_i}$, $\mathbf{b}_i \in \mathbb{R}^{r_i}$, and r_i and n_i are called the ‘‘fan-out’’ and ‘‘fan-in’’ number of the layer respectively (He et al., 2015b). This is straightforward for a fully-connected layer, and for a convolutional layer with kernel size k , c_{in} input channels and c_{out} output channels, we can still view the convolution as an affine transformation with $n_i = k^2 c_{\text{in}}$ and $r_i = c_{\text{out}}$. In particular, we use $\mathbf{h}_0 = \mathbf{x} + \delta$ to denote the input layer perturbed by δ (\mathbf{z}_0 is not applicable).

For IBP (Mirman et al., 2018; Goyal et al., 2018), it computes and propagates lower and upper bound intervals layer by layer until the last layer or the verification objective. For pre-activation \mathbf{h}_i , its interval bounds can be denoted as $[\underline{\mathbf{h}}_i, \bar{\mathbf{h}}_i]$, where $\underline{\mathbf{h}}_i \leq \mathbf{h}_i \leq \bar{\mathbf{h}}_i$ ($\forall \|\delta\|_\infty \leq \epsilon$). Similarly, there are also post-activation interval bounds $[\underline{\mathbf{z}}_i, \bar{\mathbf{z}}_i]$. Finally Eq. (2) can be verified by checking the lower bound of $[f_\theta(\mathbf{x} + \delta)]_y - [f_\theta(\mathbf{x} + \delta)]_i$.

3.2 Issues in Existing Certified Robust Training

In this section, we analyze the issues in existing IBP training. In particular, we identify two issues, including exploded bounds at initialization, and also the imbalance between ReLU activation states.

3.2.1 Exploded Bounds at Initialization

For simplicity, we assume the network has a feedforward architecture in this analysis, but the analysis can also be easily extended to other architectures. For affine layer $\mathbf{h}_i = \mathbf{W}_i \mathbf{z}_{i-1} + \mathbf{b}_i$, the IBP bound computation is as follows:

$$\underline{\mathbf{h}}_i = \mathbf{W}_{i,+} \underline{\mathbf{z}}_{i-1} + \mathbf{W}_{i,-} \bar{\mathbf{z}}_{i-1} + \mathbf{b}_i, \quad \bar{\mathbf{h}}_i = \mathbf{W}_{i,+} \bar{\mathbf{z}}_{i-1} + \mathbf{W}_{i,-} \underline{\mathbf{z}}_{i-1} + \mathbf{b}_i, \quad (3)$$

where $\mathbf{W}_{i,+}$ stands for retaining positive elements in \mathbf{W}_i only while setting other elements to zero, and vice versa for $\mathbf{W}_{i,-}$. \mathbf{h}_i can be viewed as a function with the post-activation value of the previous layer \mathbf{z}_i as input, denoted as $\mathbf{h}_i(\mathbf{z}_i)$. In Eq. (3), the IBP bounds guarantee that $\underline{\mathbf{h}}_i \leq \mathbf{h}_i(\mathbf{z}_i) \leq \bar{\mathbf{h}}_i$ ($\forall \underline{\mathbf{z}}_i \leq \mathbf{z}_i \leq \bar{\mathbf{z}}_i$) for element-wise ‘‘ \leq ’’.

We then check the tightness of the interval bounds:

$$\Delta_i = \bar{\mathbf{h}}_i - \underline{\mathbf{h}}_i = |\mathbf{W}_i|(\bar{\mathbf{z}}_{i-1} - \underline{\mathbf{z}}_{i-1}) = |\mathbf{W}_i| \delta_{i-1}, \quad (4)$$

where Δ_i denotes the gap between the upper and lower bounds, which can reflect the tightness of the bounds, and $|\mathbf{W}_i|$ stands for taking the absolute value element-wise. At initialization, we assume that each \mathbf{W}_i independently follows a distribution with zero mean and variance σ_i^2 , and the distribution is symmetric about 0. For a vector or matrix with independent elements following the same distribution, we use $\mathbb{E}(\cdot)$ to denote the expectation of this distribution. We can view each element in vector Δ_i as a random variable that follows the same distribution, and we denote its expectation as $\mathbb{E}(\Delta_i)$, to measure the expected tightness at layer i . As \mathbf{W}_i and δ_{i-1} are independent, we have $\mathbb{E}(\Delta_i) = n_i \mathbb{E}(|\mathbf{W}_i|) \mathbb{E}(\delta_{i-1})$. Detailed in Appendix D.1, we further have $\mathbb{E}(\delta_i) = \mathbb{E}(\text{ReLU}(\bar{\mathbf{h}}_i) - \text{ReLU}(\underline{\mathbf{h}}_i)) = \frac{1}{2} \mathbb{E}(\Delta_i)$, and

$$\mathbb{E}(\Delta_i) = \frac{n_i}{2} \mathbb{E}(|\mathbf{W}_i|) \mathbb{E}(\Delta_{i-1}). \quad (5)$$

Empirically, we can estimate $\mathbb{E}(\Delta_i)$ given a batch of concrete data, by taking the mean, and we use $\hat{\mathbb{E}}(\Delta_i)$ to denote the result of the empirical estimation.

We define a metric to characterize to what extent the certified bounds become looser, after propagating bounds from layer $i - 1$ to layer i :

Definition 1. We define the difference gain when bounds are propagated from layer $i - 1$ to layer i :

$$\mathbb{E}(\Delta_i) / \mathbb{E}(\Delta_{i-1}) = \frac{n_i}{2} \mathbb{E}(|\mathbf{W}_i|). \quad (6)$$

Bounds are considered to be stable if the difference gain $\mathbb{E}(\Delta_i) / \mathbb{E}(\Delta_{i-1})$ is close to 1.

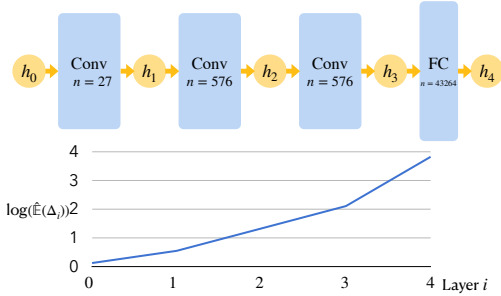


Figure 1: We show that certified bounds explode at initialization, in a simple untrained CNN (the classification layer is omitted) using Xavier initialization. We plot $\log \hat{\mathbb{E}}(\Delta_i)$ for each layer i .

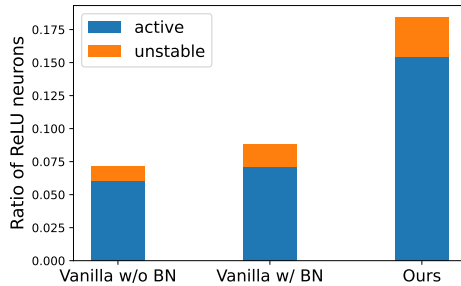


Figure 2: Ratios of active and unstable ReLU neurons for CNN-7 on CIFAR-10 with different settings. The vanilla ones are not regularized, and “vanilla (w/o BN)” does not use BN either.

A large difference gain indicates exploded bounds, but it cannot be much smaller than 1 either to avoid signal vanishing in the model. We find that weight initialization in prior works have large difference gain values especially for layers with larger n_i . For example, for the widely used Xavier initialization (Glorot & Bengio, 2010), the difference gain is $\frac{1}{4}\sqrt{n_i}$, and it can be as large as 45.25 when $n_i = 32768$ for a fully-connected layer in experiments. This indicates that certified bounds explode at initialization. We illustrate the bound explosion in Figure 1, and in Appendix A, we list the difference gain of each existing initialization method in Table 5. As a result, long warmup schedules are important in previous works, to gradually tighten certified bounds and ease training, but this is inefficient.

3.2.2 Imbalanced ReLU Activation States

We show another issue in existing certified training, where the models have a bias towards *inactive ReLU neurons*. Here “inactive ReLU neurons” are defined as neurons with non-positive pre-activation upper bounds ($\bar{\mathbf{h}}_{i,j} \leq 0$), i.e., they are always inactive regardless of input perturbations. Similarly, *active ReLU neurons* have non-negative pre-activation lower bounds ($\underline{\mathbf{h}}_{i,j} \geq 0$). There are also *unstable ReLU neurons* with uncertain activation states given different input perturbations ($\underline{\mathbf{h}}_{i,j} \leq 0 \leq \bar{\mathbf{h}}_{i,j}$). In IBP training, inactive neurons have tighter bounds than active and unstable ones as shown in Figure 5 in Appendix B, and thus the optimization tends to push the neurons to be inactive. We show this imbalance ReLU status in Figure 2 (vanilla w/o BN), and it is more severe when the warmup is shorter as shown in Appendix B.7. Too many inactive neurons indicates that many neurons are essentially unused or dead, which will harm the model’s capacity and block gradients as discussed by Lu et al. (2019) on standard training.

3.3 The Proposed Method

To address the aforementioned issues, we propose our method in three parts: 1) We derive a new weight initialization for IBP training to stabilize the tightness of bounds at initialization; 2) We propose to fully add BN to mitigate the ReLU imbalance and stabilize the variance of bounds, while models in prior works did not have BN for some or all the layers. 3) We further propose regularizations to explicitly stabilize the tightness and the balance of ReLU states during warmup.

3.3.1 IBP initialization

We propose a new *IBP initialization* for IBP training. Specifically, we independently initialize each element in \mathbf{W}_i following a normal distribution $\mathcal{N}(0, \sigma_i^2)$, and we aim to choose a value for σ_i such that the *difference gain* defined in Eq. (6) is exactly 1. When elements in \mathbf{W}_i follow the normal distribution, we have $\mathbb{E}(|\mathbf{W}_i|) = \sqrt{2/\pi}\sigma_i$, and thereby we take $\sigma_i = \frac{\sqrt{2\pi}}{n_i}$, which makes the difference gain $\frac{n_i}{2}\mathbb{E}(|\mathbf{W}_i|)$ exactly 1. This initialization can further be calibrated for non-feedforward networks such as ResNet as we discuss in Appendix A.3.

3.3.2 Batch Normalization

Batch normalization (BN) (Ioffe & Szegedy, 2015) normalizes the input of each layer to a distribution with stable mean and variance. It can improve the optimization for DNN as shown in prior works for standard DNN training (Ioffe & Szegedy, 2015; Van Laarhoven, 2017; Santurkar et al., 2018). In addition, for IBP training, BN can normalize the variance of bounds, and it can also improve the balance of ReLU activation states by shifting the center of upper and lower bounds to zero (before the additional linear transformation which comes after the normalization). In prior certified training works (Gowal et al., 2018; Zhang et al., 2020; Xu et al., 2020), they only used BN for some layers in some models but not all layers, and they did not identify the benefit of BN in certified training. We empirically demonstrate that fully adding BN to each affine layer can significantly mitigate the imbalance ReLU issue and improve IBP training. We follow the BN implementation by Wong et al. (2018); Xu et al. (2020) for certified training, where the shifting and scaling parameters are computed from unperturbed data.

Note that our previous analysis on IBP initialization considers a network without BN. BN which rescales the output of each layer can still affect the tightness of IBP bounds, and the effect of IBP initialization may be weakened. This is a limitation of the proposed initialization which could possibly be improved by considering the effect of BN in future work. Nevertheless, in Appendix A.4, we empirically show that BN still does not cancel out the effect of IBP initialization.

3.3.3 Warmup Regularization

To further address the aforementioned two issues in Sec. 3.2, and to explicitly stabilize the tightness of certified bounds and balance ReLU neuron states, we add two regularizers in the warmup stage of IBP training. The regularizers are principled and motivated by the two issues we discover.

Bound tightness regularizer Similar to the goal of stabilizing certified bounds at initialization, we also expect to keep the mean value of Δ_i in the current batch, $\hat{\mathbb{E}}(\Delta_i)$, stable along the warmup. Note that $\hat{\mathbb{E}}(\Delta_i)$ is empirically computed from a concrete batch and different from the expectation $\mathbb{E}(\Delta_i)$ at initialization. In the initialization, we aim to make $\mathbb{E}(\Delta_i) \approx \mathbb{E}(\Delta_{i-1})$. Here, we relax the goal to making $\tau \hat{\mathbb{E}}(\Delta_i) \leq \hat{\mathbb{E}}(\Delta_0)$ with a configurable tolerance value τ ($0 < \tau \leq 1$), to balance the regularization power and the model capacity. We add the following regularization term:

$$\mathcal{L}_{\text{tightness}} = \frac{1}{\tau m} \sum_{i=1}^m \text{ReLU}(\tau - \frac{\hat{\mathbb{E}}(\Delta_0)}{\hat{\mathbb{E}}(\Delta_i)}), \quad (7)$$

where the training is penalized only when $\tau \hat{\mathbb{E}}(\Delta_i) > \hat{\mathbb{E}}(\Delta_0)$ due to the clipping effect by $\text{ReLU}(\cdot)$.

ReLU activation states balancing regularizer To balance ReLU activation states, we expect to balance the impact of active ReLU neurons and inactive neurons respectively. Here, we consider the center of the interval bound, $\mathbf{c}_i = (\underline{\mathbf{h}}_i + \bar{\mathbf{h}}_i)/2$, and we model the impact as the contribution of each type of neurons to the mean and variance of the whole layer, i.e., $\mathbb{E}(\mathbf{c}_i)$ and $\text{Var}(\mathbf{c}_i)$ respectively. Note that in the beginning almost all neurons are unstable, and gradually most neurons become either active or inactive. Therefore, we add this regularizer only when there is at least one active neuron and one inactive neuron, which generally holds true unless at the training start. We use α_i to denote the ratio between the contribution of the active neurons and inactive neurons respectively to $\hat{\mathbb{E}}(\mathbf{c}_i)$, and similarly we use β_i to denote the ratio of contribution to $\text{Var}(\mathbf{c}_i)$. They are computed as:

$$\alpha_i = \frac{\sum_j \mathbb{I}(\underline{\mathbf{h}}_{i,j} > 0) \mathbf{c}_{i,j}}{-\sum_j \mathbb{I}(\bar{\mathbf{h}}_{i,j} < 0) \mathbf{c}_{i,j}}, \quad \beta_i = \frac{\sum_j \mathbb{I}(\underline{\mathbf{h}}_{i,j} > 0) (\mathbf{c}_{i,j} - \hat{\mathbb{E}}(\mathbf{c}_i))^2}{\sum_j \mathbb{I}(\bar{\mathbf{h}}_{i,j} < 0) (\mathbf{c}_{i,j} - \hat{\mathbb{E}}(\mathbf{c}_i))^2},$$

and in general $\alpha_i, \beta_i > 0$. We regard that the activation states are roughly balanced if α_i and β_i are close to 1. With the same aforementioned tolerance τ , we expect to make $\tau \leq \alpha_i, \beta_i \leq 1/\tau$, which is equivalent to making $\min(\alpha_i, 1/\alpha_i) \geq \tau$, $\min(\beta_i, 1/\beta_i) \geq \tau$. Thereby we design the following regularization term:

$$\mathcal{L}_{\text{relu}} = \frac{1}{\tau m} \sum_{i=1}^m \left(\text{ReLU}(\tau - \min(\alpha_i, \frac{1}{\alpha_i})) + \text{ReLU}(\tau - \min(\beta_i, \frac{1}{\beta_i})) \right). \quad (8)$$

3.4 Training Objectives

Certified robust training solves the robust optimization problem as Eq. (1), and when the inner maximization is verifiably solved, the base training objective without regularization is:

$$\mathcal{L}_{\text{rob}} = \bar{L}(f_{\theta}, \mathbf{x}, y, \epsilon), \quad \text{where } \bar{L}(f_{\theta}, \mathbf{x}, y, \epsilon) \geq \max_{\|\delta\|_{\infty} \leq \epsilon} L(f_{\theta}(\mathbf{x} + \delta), y), \quad (9)$$

such that $\bar{L}(f_{\theta}, \mathbf{x}, y, \epsilon)$ is an upper bound of $L(f_{\theta}(\mathbf{x} + \delta), y)$ given by a robustness verifier, e.g., IBP. In our proposed method, we first initialize the parameters with our IBP initialization, and then we perform a *short* warmup with gradually increasing ϵ ($0 \leq \epsilon \leq \epsilon_{\text{target}}$), where ϵ_{target} stands for the target perturbation radius that is usually equal to or slightly larger than the maximum perturbation radius used for test. Our training objective \mathcal{L} combines the ordinary objective Eq. (9) and the proposed regularizers:

$$\mathcal{L} = \mathcal{L}_{\text{rob}} + \lambda(\mathcal{L}_{\text{tightness}} + \mathcal{L}_{\text{relu}}), \quad (10)$$

where λ is for balancing the regularizers and the original \mathcal{L}_{rob} loss. For simplicity and efficiency, we use IBP to compute the bounds in \mathcal{L}_{rob} and the regularizers. During warmup, we also gradually decrease λ from λ_0 to 0 as ϵ grows, where $\lambda = \lambda_0(1 - \epsilon/\epsilon_{\text{target}})$. After warmup, we only use $\mathcal{L} = \mathcal{L}_{\text{rob}}$ for final training with ϵ_{target} . Note that in the regularizers, the value of each $\text{ReLU}(\cdot)$ term has the same range $[0, \tau]$, and thus in Eq. (10) we directly sum up them without weighing them for simplicity. In test, we still only use pure IBP bounds without any other tighter method.

4 Experiments

In the experiments, we demonstrate the effectiveness of our proposed method for training certifiably robust neural networks more efficiently while achieving better or comparable verified errors.

4.1 Settings

We adopt three datasets, MNIST (LeCun et al., 2010), CIFAR-10 (Krizhevsky et al., 2009) and TinyImageNet (Le & Yang, 2015). Following Xu et al. (2020), we consider three model architectures: a 7-layer feedforward convolutional network (CNN-7), Wide-ResNet (Zagoruyko & Komodakis, 2016) and ResNeXt (Xie et al., 2017). According our discussion in Sec. 3.3.2, we also modify the models to fully add a BN after every convolutional or fully-connected layer. For target perturbation radii, we mainly use $\epsilon_{\text{target}} = 0.4$ for MNIST, $\epsilon_{\text{target}} = 8/255$ for CIFAR-10, and $\epsilon_{\text{target}} = 1/255$ for TinyImageNet, following prior works, and we provide results on other perturbation radii in Appendix B.3. We provide more implementation details in Appendix C. We mainly compare with the following SOTA baselines on all the settings (note that in our main results, we also make these baselines use models with full BNs unless otherwise indicated):

- Vanilla IBP (Gowal et al., 2018) with existing initialization and no warmup regularizer. We use the default Xavier initialization in PyTorch, and we find that orthogonal initialization originally used by Gowal et al. (2018) does not improve the performance here.
- CROWN-IBP (Zhang et al., 2020) with linear relaxation bounds by CROWN (Zhang et al., 2018) during warmup. We use the generalized and accelerated version with loss fusion by Xu et al. (2020), while the original version is $O(K)$ (the number of classes) more costly. During the warmup, it combines bounds by IBP and linear relaxation with weight $\epsilon/\epsilon_{\text{target}}$ and $(1 - \epsilon/\epsilon_{\text{target}})$ respectively.

4.2 Certified Robust Training with Short Warmup

We conduct certified robust training using relatively short warmup schedules to demonstrate the effectiveness of our proposed techniques for fast training. We show the results in Table 1 for MNIST, CIFAR-10 and Table 2 for TinyImageNet. Compared to Vanilla IBP and CROWN-IBP, our improved IBP training consistently achieves lower standard errors and verified errors under same schedules respectively, where BN is added to the models for all these three training methods. We find that CROWN-IBP with loss fusion (Xu et al., 2020) tends to require a larger number of epochs to obtain good results and it sometimes underperform Vanilla IBP under short schedules, but disabling loss fusion can make it much more costly and unscalable. In terms of the best results, we achieve verified error 10.82% on MNIST $\epsilon_{\text{target}} = 0.4$, 65.03% on CIFAR-10 $\epsilon_{\text{target}} = 8/255$, and 82.36% on

Table 1: Standard and verified error rates (%) of models trained with different methods respectively on MNIST ($\epsilon_{\text{target}} = 0.4$) and CIFAR-10 ($\epsilon_{\text{target}} = 8/255$). Schedule is represented as the total number of epochs and the number of epochs in each of the three phases with $\epsilon = 0$, increasing $\epsilon \in (0, \epsilon_{\text{target}})$ and final $\epsilon = \epsilon_{\text{target}}$ respectively. We report the mean and standard deviation of the results on 5 repeats for CNN-7 and 3 repeats for Wide-ResNet and ResNeXt respectively. All models include BN after every layer (see Sec. 3.3.2). We also report the best run in “Ours (best)” since main results in prior works did not have repeats. Literature results with the “†” mark are concurrent works.

Dataset	Schedule (epochs)	Method	CNN-7 (with full BN)		Wide-ResNet (with full BN)		ResNeXt (with full BN)	
			Standard	Verified	Standard	Verified	Standard	Verified
MNIST	70 (0+20+50)	Vanilla IBP	2.59 ± 0.06	12.03 ± 0.09	3.18 ± 0.05	12.93 ± 0.17	4.09 ± 0.46	15.36 ± 0.94
		CROWN-IBP ^a	2.75 ± 0.12	12.04 ± 0.22	3.39 ± 0.05	13.10 ± 0.15	4.22 ± 0.53	15.24 ± 0.78
		Ours	2.33 ± 0.08	11.03 ± 0.13	2.77 ± 0.02	11.76 ± 0.07	3.22 ± 0.08	13.43 ± 0.17
		Ours (best)	2.20	10.82	2.75	11.69	3.17	13.20
	Literature results		Warmup		Total (epochs)		Standard	Verified
	Gowal et al. (2018)		(2K+10K) steps		100		1.66	15.01 ^b
	Zhang et al. (2020)		(9 + 51) epochs		200		2.17	12.06
	†IBP+ParamRamp (Lyu et al., 2021) ^c		(9 + 51) epochs		200		2.16	10.88
	†CROWN-IBP+ParamRamp (Lyu et al., 2021) ^c		(9 + 51) epochs		200		2.36	10.61
	CIFAR-10	70 (1+20+49)	Vanilla IBP	58.72 ± 0.27	69.88 ± 0.10	58.85 ± 0.22	69.77 ± 0.32	60.10 ± 0.27
CROWN-IBP ^a			63.19 ± 0.36	71.29 ± 0.19	62.76 ± 0.23	71.82 ± 0.30	64.75 ± 0.50	72.50 ± 0.20
Ours			56.64 ± 0.48	68.81 ± 0.24	56.74 ± 0.40	68.71 ± 0.29	59.33 ± 0.86	70.62 ± 0.59
160 (1+80+79)		Vanilla IBP	53.80 ± 0.71	67.01 ± 0.29	54.31 ± 0.46	67.45 ± 0.21	55.23 ± 0.12	68.28 ± 0.15
		CROWN-IBP ^a	58.76 ± 0.76	69.67 ± 0.38	60.39 ± 0.33	70.07 ± 0.42	61.08 ± 0.35	71.26 ± 0.11
		Ours	51.72 ± 0.40	65.58 ± 0.32	51.95 ± 0.27	65.91 ± 0.14	53.68 ± 0.33	66.91 ± 0.40
		Ours (best)	51.06	65.03	51.63	65.72	53.38	66.41
Literature results		Warmup		Total (epochs)		Standard	Verified	
Gowal et al. (2018)		(5K+50K) steps		3,200		50.51	68.44 ^c	
Zhang et al. (2020)		(320 + 1600) epochs		3,200		54.02	66.94	
Balunovic & Vechev (2020)		N/A ^d		800		48.3	72.5	
Xu et al. (2020)		(100 + 800) epochs		2,000		53.71	66.62	
†IBP+ParamRamp (Lyu et al., 2021) ^e		(320 + 1600) epochs		3,200		55.28	67.09	
†CROWN-IBP+ParamRamp (Lyu et al., 2021) ^e		(320 + 1600) epochs		3,200		51.94	65.08	
† ℓ_∞ -dist net (other architecture) (Zhang et al., 2021) ^f		N/A ^f		800		48.32	64.90	

^a CROWN-IBP here follows Xu et al. (2020) with loss fusion for efficiency, but we found it does not perform well with a short training schedule under our settings and usually requires a longer schedule to achieve good results.

^b Some test results in Gowal et al. (2018) are obtained with costly mixed integer programming (MIP) and linear programming (LP); we take IBP verified errors for fair comparison following Zhang et al. (2020).

^c Additional PGD adversarial training was involved for this result, according to Zhang et al. (2020).

^d Balunovic & Vechev (2020) used a different training scheme and train the network layer by layer.

^e Lyu et al. (2021) use IBP-based and CROWN-IBP-based training respectively with their parameterized activation, and they use a tighter linear bound propagation method for testing instead of IBP.

^f Zhang et al. (2021) use a very different model architecture with ℓ_∞ distance neurons rather than traditional DNNs, but still need a long schedule on both ϵ and ℓ_p norm where p is gradually increased until ∞ .

Table 2: Standard and verified error rates (%) on TinyImageNet ($\epsilon_t = 1/255$). The best result in literature (Xu et al., 2020) has a standard error of 72.18% and verified error of 84.14% using 800 epochs. We achieve 82.36% verified error using only 80 epochs.

Model (with full BN)	Schedule (epochs)	Vanilla IBP		CROWN-IBP		Ours	
		Standard	Verified	Standard	Verified	Standard	Verified
CNN-7	80 (1+10+69)	75.50	82.92	76.00	82.81	75.20	82.45
	80 (1+20+59)	74.68	82.84	76.27	83.35	74.29	82.36
Wide-ResNet ^a	80 (1+10+69)	75.89	83.00	75.85	83.65	74.90	82.49
	80 (1+20+59)	75.65	83.17	75.95	83.08	74.59	82.75
ResNeXt	80(1+10+69)	82.39	87.15	85.47	89.11	80.20	85.77
	80 (1+20+59)	81.72	87.10	80.81	86.43	78.91	85.78

^a The Wide-ResNet model used here is 5 times smaller than the one used in Xu et al. (2020) to save training time. Additionally, we include BN after every layer in all models (see Section 3.3.2).

TinyImageNet $\epsilon_{\text{target}} = 1/255$, which makes a notable improvement over literature SOTA (Gowal et al., 2018; Xu et al., 2020) that used long training schedules. Compared to concurrent works (Lyu et al., 2021; Zhang et al., 2021) which use different improvement techniques, we have comparable verified errors, but they still need long training schedules. For reference, we tried Zhang et al. (2021) which used a different architecture with “ ℓ_∞ distance neurons” rather than convolution-based DNNs. On CIFAR-10 using 160 total epochs by reducing their training schedule proportionally, their verified error is 68.44% which is much higher than ours. Overall, the results demonstrate that our improved IBP training is effective for more efficient certified robust training with a shorter warmup.

4.3 Comparison on Training Cost

Table 3: Comparison of estimated time cost (seconds), for CNN-7 on CIFAR-10. We report the total time, and also the per-epoch time during three training phases of ϵ schedule for methods with a short warmup. Literature results with the “†” mark are considered as concurrent.

Method	Epochs	Epoch time in each phase (s)			Total time (s)
		0	(0, ϵ_{target})	ϵ_{target}	
Literature Results	IBP (Gowal et al., 2018)	3200			40496×4^a
	CROWN-IBP (w/o loss fusion) (Zhang et al., 2020)	3200	-		91288×4^a
	CROWN-IBP (Xu et al., 2020)	2000			52362×4^a
	†IBP+ParamRamp (Lyu et al., 2021)	3200			$40496 \times 4 \times 1.09^b$
	†CROWN-IBP+ParamRamp (Lyu et al., 2021)	3200			$91288 \times 4 \times 1.51^b$
Short Warmup	Vanilla IBP	160	30.0	54.8	8747.9
	CROWN-IBP	160	30.0	78.5	10641.3
	Ours	160	64.0	64.0	9512.3

^a 4 GPUs were used and their models are slightly different (we add BN after every layer).

^b The factors 1.09 and 1.51 are the overhead of their method reported by (Lyu et al., 2021) when combining with IBP or CROWN-IBP.

We compare the training cost using a single NVIDIA RTX 2080 Ti GPU. For methods using short warmup, we measure the per-epoch time cost during three different phases, namely $\epsilon = 0$, $0 < \epsilon < \epsilon_{\text{target}}$, and $\epsilon = \epsilon_{\text{target}}$, and we then estimate the total training time according to the schedule. We use gradient accumulation wherever needed to fit the training into the memory of a single GPU. We also compare with total time cost with literature methods using long schedules. We show the results of CNN-7 for CIFAR-10 in Table 3, and other settings in Appendix B.1. For $\epsilon = 0$, Vanilla IBP and CROWN-IBP use regular training while we compute IBP bounds for regularization and have a small overhead, but this phase is extremely short (no more than 1 epoch here). For $0 < \epsilon < \epsilon_{\text{target}}$, our method has a small overhead on regularizers compared to Vanilla IBP, while CROWN-IBP using linear relaxation can be more costly. For $\epsilon = \epsilon_{\text{target}}$, all the three methods use the same pure IBP.

For total time on CIFAR-10 with the same 160-epoch schedule, we only have a small overhead of around 9% ~ 13% compared to Vanilla IBP and the cost is still around 12% ~ 23% lower than CROWN-IBP, while we achieve lower verified errors than the baselines under such short warmup schedules (see Table 1). And importantly, compared to literature using long training schedules, we significantly reduce the number of training epochs and the total training time (e.g., Xu et al. (2020) is around 20× more costly than ours in total).

4.4 Ablation Study and Discussions

In this section, we empirically verify whether each part of our modification contributes to the improvement and whether they behave as we expect. We conduct an ablation study and also plot the curve of the regularization terms to reflect the bound tightness and ReLU balance during training.

We use CIFAR-10 with the currently best CNN-7 model under the “1 + 20” and “1 + 80” warmup schedules as used in Table 1. We report the results in Table 4. The first three rows show that fully adding BN improves the training when vanilla IBP is used, and it is important to add BN for the fully-connected layer, which was missed in prior works. Based on the improved model structure, adding both IBP initialization and warmup regularization further improves the performance, and removing either of these parts leads to a degraded performance.

We notice that adding IBP initialization without warmup regularization may not improve the verified error. A factor is that IBP initialization can reduce the variance of the outputs (see Appendix D.2), and it may harm the training during the early warmup, when ϵ is small and certified training is close to standard training. Also, the effect of initialization can be weakened when ϵ is much smaller than ϵ_{target} . But the warmup regularization can continue to tighten the bounds, and the IBP initialization can benefit the optimization for the tightness regularizer. Nevertheless, IBP initialization is more beneficial for deep models where the exploded bound issue is more severe (see Appendix B.8).

It is also important to fully add BN to make the warmup regularization work well. BN can normalize the variance of the layers, so the tightness regularizer can more effectively tighten certified bounds w.r.t. the stable variance; otherwise the training may trivially optimize tightness regularizer by making the magnitude of the network output small.

Table 4: Standard error and verified error rates (%) in the ablation study with CNN-7 on CIFAR-10. “BN-Conv” stands for BN after each convolutions, and “BN-FC” stands for BN after the hidden fully-connected layer. “✓” means that the component is enabled, and “×” means that the component is disabled. We repeat each setting for 5 times and report the mean and standard deviation.

BN-Conv	BN-FC	IBP Initialization	$\mathcal{L}_{\text{tightness}}$	$\mathcal{L}_{\text{relu}}$	70 (1+20+49) epochs		160 (1+80+79) epochs	
					Standard	Verified	Standard	Verified
×	×	×	×	×	59.33±0.70	70.18±0.18	57.08±0.29	69.43±0.28
✓	×	×	×	×	61.95±0.80	71.12±0.42	57.21±0.65	69.21±0.30
✓	✓	×	×	×	58.72±0.27	69.88±0.10	53.80±0.71	67.01±0.29
✓	✓	✓	×	×	58.93±0.29	69.60±0.35	54.59±0.64	67.63±0.34
✓	✓	✓	✓	×	56.76±0.38	68.96±0.49	53.08±0.26	66.74±0.20
✓	✓	✓	×	✓	58.49±0.42	69.38±0.23	53.29±0.76	66.46±0.44
✓	✓	×	✓	✓	58.79±0.40	69.29±0.28	52.45±0.34	66.34±0.38
✓	✓	✓	✓	✓	56.64±0.48	68.81±0.24	51.72±0.40	65.58±0.32

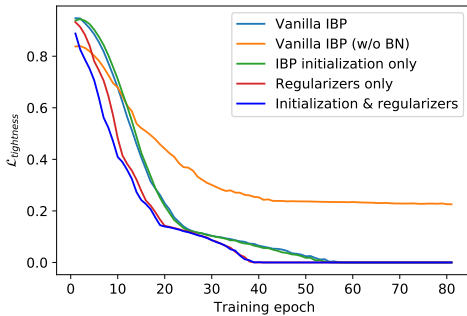


Figure 3: $\mathcal{L}_{\text{tightness}}$ during warmup. $\mathcal{L}_{\text{tightness}}$ is optimized only for “regularizers only” and “initialization & regularizers” setting, and BN is fully added to every layer except for “Vanilla IBP (w/o BN)”.

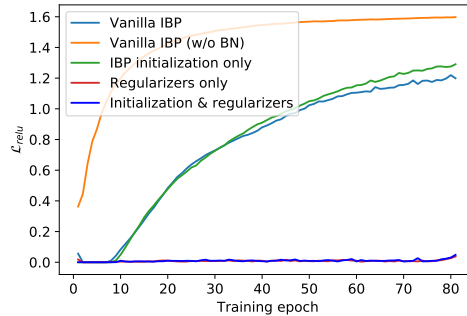


Figure 4: $\mathcal{L}_{\text{relu}}$ during warmup, under same setting as in Figure 3.

Finally, we also plot the training curves of the regularizers to confirm if the regularizers are effectively optimized, so that the bound tightness and ReLU balance are indeed improved. Note that for the settings without regularizers, we only plot but not optimize the regularizers. In Figure 3, we plot $\mathcal{L}_{\text{tightness}}$. By using the regularization in training, $\mathcal{L}_{\text{tightness}}$ descends faster, and further adding the IBP initialization leads to even faster descent during the early epochs. In Figure 4, we show that the $\mathcal{L}_{\text{relu}}$ is indeed under control when we optimize it, while $\mathcal{L}_{\text{relu}}$ could gradually grow larger when it is not added in training. Notably, when BN is removed and the regularization term is not optimized (Vanilla IBP (w/o BN)), $\mathcal{L}_{\text{relu}}$ becomes extremely large in later epochs, and $\mathcal{L}_{\text{tightness}}$ is also large in the end, which suggests that the training is hampered.

5 Conclusion

In this paper, we identify two issues in existing certified robust training methods regarding exploded bounds and imbalanced ReLU neuron states. To address these issues based on IBP training, we propose an IBP initialization and warmup regularization, and we also identify the benefit of fully adding BN. With our improvements, we demonstrate that we are able to achieve better verified errors using much shorter warmup and training schedules compared to literatures under the same convolution-based network architecture, for fast certified robust training.

Acknowledgement

This work is supported in part by NSF under IIS-1901527, IIS-2008173, IIS-2048280 and by Army Research Laboratory under agreement number W911NF-20-2-0158.

References

- Abadi, M., Agarwal, A., Barham, P., Brevdo, E., Chen, Z., Citro, C., Corrado, G. S., Davis, A., Dean, J., Devin, M., Ghemawat, S., Goodfellow, I., Harp, A., Irving, G., Isard, M., Jia, Y., Jozefowicz, R., Kaiser, L., Kudlur, M., Levenberg, J., Mane, D., Monga, R., Moore, S., Murray, D., Olah, C., Schuster, M., Shlens, J., Steiner, B., Sutskever, I., Talwar, K., Tucker, P., Vanhoucke, V., Vasudevan, V., Viegas, F., Vinyals, O., Warden, P., Wattenberg, M., Wicke, M., Yu, Y., and Zheng, X. Tensorflow: Large-scale machine learning on heterogeneous distributed systems, 2016.
- Arpit, D., Campos, V., and Bengio, Y. How to initialize your network? robust initialization for weightnorm & resnets. In Wallach, H., Larochelle, H., Beygelzimer, A., d'Alché-Buc, F., Fox, E., and Garnett, R. (eds.), *Advances in Neural Information Processing Systems*, volume 32. Curran Associates, Inc., 2019. URL <https://proceedings.neurips.cc/paper/2019/file/e520f70ac3930490458892665cda6620-Paper.pdf>.
- Balunovic, M. and Vechev, M. Adversarial training and provable defenses: Bridging the gap. In *International Conference on Learning Representations*, 2020.
- Bhattacharya, A. Learnable weight initialization in neural networks. 2020.
- Blum, A., Dick, T., Manoj, N., and Zhang, H. Random smoothing might be unable to certify ℓ_∞ robustness for high-dimensional images. *Journal of Machine Learning Research*, 21:1–21, 2020.
- Bunel, R., Turkaslan, I., Torr, P. H. S., Kohli, P., and Kumar, M. P. Piecewise linear neural network verification: A comparative study. *CoRR*, abs/1711.00455, 2017. URL <http://arxiv.org/abs/1711.00455>.
- Carlini, N. and Wagner, D. Adversarial examples are not easily detected: Bypassing ten detection methods. In *Proceedings of the 10th ACM Workshop on Artificial Intelligence and Security*, pp. 3–14. ACM, 2017.
- Chen, H., Zhang, H., Chen, P.-Y., Yi, J., and Hsieh, C.-J. Attacking visual language grounding with adversarial examples: A case study on neural image captioning. *arXiv preprint arXiv:1712.02051*, 2017.
- Choi, J.-H., Zhang, H., Kim, J.-H., Hsieh, C.-J., and Lee, J.-S. Evaluating robustness of deep image super-resolution against adversarial attacks. In *Proceedings of the IEEE/CVF International Conference on Computer Vision*, pp. 303–311, 2019.
- Cohen, J. M., Rosenfeld, E., and Kolter, J. Z. Certified adversarial robustness via randomized smoothing. In *ICML*, 2019.
- Dvijotham, K., Goyal, S., Stanforth, R., Arandjelovic, R., O’Donoghue, B., Uesato, J., and Kohli, P. Training verified learners with learned verifiers. *arXiv preprint arXiv:1805.10265*, 2018.
- Glorot, X. and Bengio, Y. Understanding the difficulty of training deep feedforward neural networks. In Teh, Y. W. and Titterton, M. (eds.), *Proceedings of the Thirteenth International Conference on Artificial Intelligence and Statistics*, volume 9 of *Proceedings of Machine Learning Research*, pp. 249–256, Chia Laguna Resort, Sardinia, Italy, 13–15 May 2010. JMLR Workshop and Conference Proceedings. URL <http://proceedings.mlr.press/v9/glorot10a.html>.
- Goodfellow, I. J., Shlens, J., and Szegedy, C. Explaining and harnessing adversarial examples. In *ICLR*, 2015.
- Goyal, S., Dvijotham, K., Stanforth, R., Bunel, R., Qin, C., Uesato, J., Mann, T., and Kohli, P. On the effectiveness of interval bound propagation for training verifiably robust models. *arXiv preprint arXiv:1810.12715*, 2018.
- Hanin, B. and Rolnick, D. How to start training: The effect of initialization and architecture. In Bengio, S., Wallach, H., Larochelle, H., Grauman, K., Cesa-Bianchi, N., and Garnett, R. (eds.), *Advances in Neural Information Processing Systems*, volume 31. Curran Associates, Inc., 2018. URL <https://proceedings.neurips.cc/paper/2018/file/d81f9c1be2e08964bf9f24b15f0e4900-Paper.pdf>.

- He, K., Zhang, X., Ren, S., and Sun, J. Delving deep into rectifiers: Surpassing human-level performance on imagenet classification. In *Proceedings of the IEEE International Conference on Computer Vision (ICCV)*, December 2015a.
- He, K., Zhang, X., Ren, S., and Sun, J. Delving deep into rectifiers: Surpassing human-level performance on imagenet classification. In *Proceedings of the IEEE International Conference on Computer Vision (ICCV)*, December 2015b.
- Huang, X. S., Perez, F., Ba, J., and Volkovs, M. Improving transformer optimization through better initialization. In III, H. D. and Singh, A. (eds.), *Proceedings of the 37th International Conference on Machine Learning*, volume 119 of *Proceedings of Machine Learning Research*, pp. 4475–4483. PMLR, 13–18 Jul 2020. URL <http://proceedings.mlr.press/v119/huang20f.html>.
- Ioffe, S. and Szegedy, C. Batch normalization: Accelerating deep network training by reducing internal covariate shift. In *International conference on machine learning*, pp. 448–456. PMLR, 2015.
- Jovanović, N., Balunović, M., Baader, M., and Vechev, M. Certified defenses: Why tighter relaxations may hurt training? *arXiv preprint arXiv:2102.06700*, 2021.
- Katz, G., Barrett, C., Dill, D. L., Julian, K., and Kochenderfer, M. J. Reluplex: An efficient smt solver for verifying deep neural networks. In *International Conference on Computer Aided Verification*, pp. 97–117. Springer, 2017.
- Kingma, D. P. and Ba, J. Adam: A method for stochastic optimization. *arXiv preprint arXiv:1412.6980*, 2014.
- Krizhevsky, A., Hinton, G., et al. Learning multiple layers of features from tiny images. *Technical Report TR-2009*, 2009.
- Kumar, A., Levine, A., Goldstein, T., and Feizi, S. Curse of dimensionality on randomized smoothing for certifiable robustness. In *International Conference on Machine Learning*, pp. 5458–5467. PMLR, 2020.
- Kurakin, A., Goodfellow, I., and Bengio, S. Adversarial examples in the physical world. *arXiv preprint arXiv:1607.02533*, 2016.
- Le, Y. and Yang, X. Tiny imagenet visual recognition challenge. *CS 231N*, 2015.
- LeCun, Y., Cortes, C., and Burges, C. Mnist handwritten digit database. *ATT Labs [Online]*. Available: <http://yann.lecun.com/exdb/mnist>, 2, 2010.
- Lecuyer, M., Atlidakis, V., Geambasu, R., Hsu, D., and Jana, S. Certified robustness to adversarial examples with differential privacy. In *2019 IEEE Symposium on Security and Privacy (SP)*, pp. 656–672. IEEE, 2019.
- Lee, S., Lee, W., Park, J., and Lee, J. Loss landscape matters: Training certifiably robust models with favorable loss landscape. 2021. URL <https://openreview.net/forum?id=lvXLfNeCQdK>.
- Li, B., Chen, C., Wang, W., and Carin, L. Certified adversarial robustness with additive noise. In *Advances in Neural Information Processing Systems*, pp. 9464–9474, 2019.
- Lu, L., Shin, Y., Su, Y., and Karniadakis, G. E. Dying relu and initialization: Theory and numerical examples. *arXiv preprint arXiv:1903.06733*, 2019.
- Lyu, Z., Guo, M., Wu, T., Xu, G., Zhang, K., and Lin, D. Towards evaluating and training verifiably robust neural networks, 2021.
- Madry, A., Makelov, A., Schmidt, L., Tsipras, D., and Vladu, A. Towards deep learning models resistant to adversarial attacks. In *ICLR*, 2018.
- Mirman, M., Gehr, T., and Vechev, M. Differentiable abstract interpretation for provably robust neural networks. In *International Conference on Machine Learning*, pp. 3575–3583, 2018.

- Paszke, A., Gross, S., Massa, F., Lerer, A., Bradbury, J., Chanan, G., Killeen, T., Lin, Z., Gimelshein, N., Antiga, L., Desmaison, A., Kopf, A., Yang, E., DeVito, Z., Raison, M., Tejani, A., Chilamkurthy, S., Steiner, B., Fang, L., Bai, J., and Chintala, S. Pytorch: An imperative style, high-performance deep learning library. In *Advances in Neural Information Processing Systems 32*, pp. 8024–8035. Curran Associates, Inc., 2019.
- Raghunathan, A., Steinhardt, J., and Liang, P. Certified defenses against adversarial examples. *International Conference on Learning Representations (ICLR)*, arXiv preprint arXiv:1801.09344, 2018a.
- Raghunathan, A., Steinhardt, J., and Liang, P. S. Semidefinite relaxations for certifying robustness to adversarial examples. In *Advances in Neural Information Processing Systems*, pp. 10877–10887, 2018b.
- Salman, H., Li, J., Razenshteyn, I., Zhang, P., Zhang, H., Bubeck, S., and Yang, G. Provably robust deep learning via adversarially trained smoothed classifiers. In *Advances in Neural Information Processing Systems*, pp. 11289–11300, 2019.
- Santurkar, S., Tsipras, D., Ilyas, A., and Madry, A. How does batch normalization help optimization? In *Proceedings of the 32nd international conference on neural information processing systems*, pp. 2488–2498, 2018.
- Saxe, A. M., McClelland, J. L., and Ganguli, S. Exact solutions to the nonlinear dynamics of learning in deep linear neural networks. arXiv preprint arXiv:1312.6120, 2013.
- Singh, G., Gehr, T., Mirman, M., Püschel, M., and Vechev, M. Fast and effective robustness certification. In *Advances in Neural Information Processing Systems*, pp. 10825–10836, 2018.
- Singh, G., Gehr, T., Püschel, M., and Vechev, M. An abstract domain for certifying neural networks. *Proceedings of the ACM on Programming Languages*, 3(POPL):41, 2019.
- Su, D., Zhang, H., Chen, H., Yi, J., Chen, P.-Y., and Gao, Y. Is robustness the cost of accuracy?—a comprehensive study on the robustness of 18 deep image classification models. In *Proceedings of the European Conference on Computer Vision (ECCV)*, pp. 631–648, 2018.
- Szegedy, C., Zaremba, W., Sutskever, I., Bruna, J., Erhan, D., Goodfellow, I., and Fergus, R. Intriguing properties of neural networks. In *ICLR*, 2013.
- Taki, M. Deep residual networks and weight initialization. *CoRR*, abs/1709.02956, 2017. URL <http://arxiv.org/abs/1709.02956>.
- Van Laarhoven, T. L2 regularization versus batch and weight normalization. arXiv preprint arXiv:1706.05350, 2017.
- Wang, S., Chen, Y., Abdou, A., and Jana, S. Mixtrain: Scalable training of formally robust neural networks. arXiv preprint arXiv:1811.02625, 2018a.
- Wang, S., Pei, K., Whitehouse, J., Yang, J., and Jana, S. Efficient formal safety analysis of neural networks. In *Advances in Neural Information Processing Systems*, pp. 6367–6377, 2018b.
- Wang, S., Zhang, H., Xu, K., Lin, X., Jana, S., Hsieh, C.-J., and Kolter, J. Z. Beta-crown: Efficient bound propagation with per-neuron split constraints for complete and incomplete neural network verification. arXiv preprint arXiv:2103.06624, 2021.
- Wong, E. and Kolter, Z. Provable defenses against adversarial examples via the convex outer adversarial polytope. In *International Conference on Machine Learning*, pp. 5283–5292, 2018.
- Wong, E., Schmidt, F., Metzen, J. H., and Kolter, J. Z. Scaling provable adversarial defenses. In *NIPS*, 2018.
- Xiao, K. Y., Tjeng, V., Shafiullah, N. M., and Madry, A. Training for faster adversarial robustness verification via inducing relu stability. In *ICLR*, 2019.

- Xie, S., Girshick, R., Dollár, P., Tu, Z., and He, K. Aggregated residual transformations for deep neural networks. In *Proceedings of the IEEE conference on computer vision and pattern recognition*, pp. 1492–1500, 2017.
- Xu, K., Shi, Z., Zhang, H., Wang, Y., Chang, K.-W., Huang, M., Kailkhura, B., Lin, X., and Hsieh, C.-J. Automatic perturbation analysis for scalable certified robustness and beyond. *Advances in Neural Information Processing Systems*, 33, 2020.
- Yang, G., Duan, T., Hu, J. E., Salman, H., Razenshteyn, I., and Li, J. Randomized smoothing of all shapes and sizes. In *International Conference on Machine Learning*, pp. 10693–10705. PMLR, 2020.
- Zagoruyko, S. and Komodakis, N. Wide residual networks. *arXiv preprint arXiv:1605.07146*, 2016.
- Zhang, B., Cai, T., Lu, Z., He, D., and Wang, L. Towards certifying ℓ_∞ robustness using neural networks with ℓ_∞ -dist neurons. *arXiv preprint arXiv:2102.05363*, 2021.
- Zhang, H., Weng, T.-W., Chen, P.-Y., Hsieh, C.-J., and Daniel, L. Efficient neural network robustness certification with general activation functions. In *Advances in neural information processing systems*, pp. 4939–4948, 2018.
- Zhang, H., Chen, H., Xiao, C., Li, B., Boning, D., and Hsieh, C.-J. Towards stable and efficient training of verifiably robust neural networks. In *International Conference on Learning Representations*, 2020.
- Zhu, C., Ni, R., Xu, Z., Kong, K., Huang, W. R., and Goldstein, T. Gradinit: Learning to initialize neural networks for stable and efficient training. *arXiv preprint arXiv:2102.08098*, 2021.

A Supplementary Illustrations for Motivation and Methodology

A.1 List of Initialization Methods in Prior Works

Table 5: List of several weight initialization methods and their *difference gain*. We show each difference gain in both closed form, and also empirical values when $n_i \in \{27, 576, 1152, 32768\}$ for a 7-layer CNN model (without BN). The concrete values are obtained by computing the mean of 100 random trials respectively. For orthogonal initialization, obtaining a closed form of difference gain is non-trivial so we omit its closed-form result, but it has large difference gains under empirical measurements.

Method	Adopted by	Closed form	Difference Gain			
			$n_i = 27$	$n_i = 576$	$n_i = 1152$	$n_i = 32768$
Xavier (uniform) (Glorot & Bengio, 2010)	Zhang et al. (2020); Xu et al. (2020)	$\frac{1}{4}\sqrt{n_i}$	1.30	6.00	8.48	45.25
Xavier (Gaussian) (Glorot & Bengio, 2010)	-	$\sqrt{\frac{1}{2\pi}}\sqrt{n_i}$	2.07	9.57	13.54	72.2
Kaiming (uniform) (He et al., 2015b)	-	$\frac{\sqrt{3}}{4}\sqrt{n_i}$	3.20	14.70	20.77	110.85
Kaiming (Gaussian) (He et al., 2015b)	-	$\sqrt{\frac{1}{\pi}}\sqrt{n_i}$	2.93	13.54	19.15	102.13
Orthogonal (Saxe et al., 2013)	Gowal et al. (2018)	-	2.09	9.58	13.54	72.22
IBP Initialization	This work	1	1.01	1.00	1.00	1.00

In Table 5, we list several weight initialization methods and their corresponding difference gain (see Def. 1). Prior weight initialization methods lead to large difference gain values especially when n_i is larger, which indicates exploded certified bounds at initialization. In contrast, our initialization yields a constant difference gain of 1 regardless of n_i .

While He et al. (2015b) proposed Kaiming initialization to stabilize the variance of each layer in standard DNN training, compared to Xavier initialization, it has even larger difference gain values and thus it tends to worsen the tightness of certified bounds here. For CNN-7 on CIFAR-10 using 160 total training epochs, if we make the Vanilla IBP baseline use Kaiming initialization, the verified error is $(68.07 \pm 0.30)\%$, which is worse than the baseline result using Xavier initialization, i.e., $(67.01 \pm 0.29)\%$. The empirical result aligns with our theoretical insight since Kaiming initialization has larger difference gain values.

A.2 Illustration of IBP Relaxations for Different Neuron States

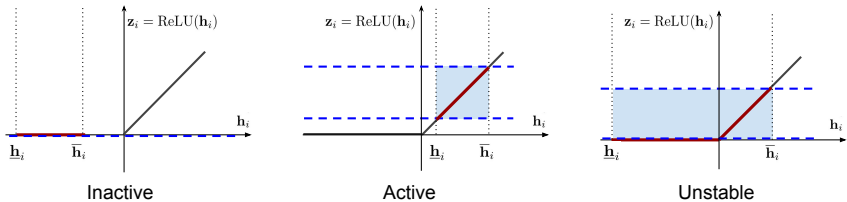


Figure 5: Three activation states of ReLU neurons determined by pre-activation lower and upper bounds and their corresponding IBP relaxations. The relaxed areas are shown in light blue.

In Figure 5, we illustrate IBP relaxations for ReLU neurons with the three different states respectively. Inactive neurons have no relaxation error compared with the other two kinds of neurons, and thus IBP training tends to prefer inactive neurons more to tighten certified bounds, compared to the other two ReLU neuron states. This leads to an imbalance in ReLU neuron states for vanilla IBP on models without BN. In this paper, we identify the benefit of fully adding BN layers to mitigate the imbalance, because BN normalizes pre-activation values. We also add a regularization to further encourage ReLU balance.

A.3 IBP Initialization for Non-feedforward Networks

Our analysis in Section 3.2.1 is based on feedforward networks but it can also be easily extended to other architectures. On the weight initialization for standard DNN training, Hanin & Rolnick (2018); Arpit et al. (2019) extended the weight initialization to ResNet, which aimed to keep the variance stable. In IBP initialization, we want to make $\mathbb{E}(\Delta_i)$ stable instead, and we give an example

on ResNet. We consider a residual connection $\tilde{\mathbf{h}}_i = \mathbf{h}_i + \mathbf{h}_{i-1}$, and we want to make its tightness $\bar{\mathbf{h}}_i + \bar{\mathbf{h}}_{i-1} - (\underline{\mathbf{h}}_i + \underline{\mathbf{h}}_{i-1})$ stable, which equals to $\Delta_i + \Delta_{i-1}$. Our IBP initialization in Section 3.3.1 makes $\mathbb{E}(\Delta_i) \approx \mathbb{E}(\Delta_{i-1})$, and thereby $\mathbb{E}(\Delta_i + \Delta_{i-1}) \approx 2\mathbb{E}(\Delta_{i-1})$. Here we get an additional growth factor of 2, when propagating bounds from layer $i - 1$ to layer i . This factor is a constant and does not depend on the fan-in number n_i . We can further remove this factor, we can divide the weight after each residual connection by 2 (this is equivalent to dividing $\tilde{\mathbf{h}}_i$ by 2 when it is used by subsequent layers).

A.4 Effect of Batch Normalization on IBP Bound Tightness

Our analysis in Section 3.2.1 does not consider BN. In this section, we analyze the tightness of certified bounds when BN presents. As mentioned in Section 3.3.2, we use mean and variance estimation computed from clean data in BN (which is also the standard way). For the output bounds $\underline{\mathbf{h}}_i$ and $\bar{\mathbf{h}}_i$, we use $\underline{\mathbf{h}}'_i$ and $\bar{\mathbf{h}}'_i$ to denote the output bounds after BN. We have $\underline{\mathbf{h}}'_i = a_i \frac{\underline{\mathbf{h}}_i - \mu(\mathbf{h}_i)}{\sigma(\mathbf{h}_i)} + b_i$, where $\mu(\mathbf{h}_i)$ and $\sigma(\mathbf{h}_i)$ stand for the estimated the mean and standard deviation respectively from clean output \mathbf{h}_i , and a_i and b_i are the weight and bias of BN. Similarly we can get $\bar{\mathbf{h}}'_i$. Therefore, to conduct a analysis similar to Sec. 3.2.1 for BN, we first need to estimate $\mu(\mathbf{h}_i)$ and $\sigma(\mathbf{h}_i)$, and then we can estimate $\bar{\mathbf{h}}'_i, \underline{\mathbf{h}}'_i$. Finally, we have $\Delta'_i = \bar{\mathbf{h}}'_i - \underline{\mathbf{h}}'_i$ to denote the bound tightness after BN.

At initialization, we assume elements in \mathbf{h}_i are independently initialized following a zero-mean Gaussian distribution, and Δ'_i can be computed from the variance of the Gaussian distribution. However, after a single step of training, elements in \mathbf{h}_i are no longer independent, and the mean and variance in BN are difficult to calculate explicitly. But we can empirically estimate them. Although when $\sigma(\mathbf{h}_i) < 1$ (which is true if we use IBP initialization to tighten certified bounds), Δ'_i will get larger than Δ_i , i.e., bounds become looser after they are propagated through BN, we can show empirically that IBP initialization is still able to tighten the bounds in this situation.

In Table 6, we compare $\log(\hat{\mathbb{E}}(\Delta_m)/\hat{\mathbb{E}}(\Delta_0))$ of CNN-7 model with full BN on CIFAR-10 during the early epochs, where m is the last layer of the model, with and without IBP initialization respectively. A smaller value indicates that the bounds are tighter. And we can see that the model with IBP initialization has smaller $\hat{\mathbb{E}}(\Delta_m)/\hat{\mathbb{E}}(\Delta_0)$ along these epochs and thus has tighter bounds.

IBP Initialization	Epoch 1	Epoch 2	Epoch 3	Epoch 4
No	16.29	15.21	13.08	11.90
Yes	11.56	12.42	11.97	11.24

Table 6: $\log(\hat{\mathbb{E}}(\Delta_m)/\hat{\mathbb{E}}(\Delta_0))$ at the first 5 epochs of CNN-7 with full BN on CIFAR-10, with and without IBP initialization respectively, which reflects the tightness of certified bounds along the training

B Additional Experiments

B.1 Computational Cost for All Datasets and Models

In addition to the time cost comparison on CNN-7 on CIFAR shown in Section 4.3, we report computation cost results for all the datasets and models in Table 7. Under same training schedules, results show that our proposed method has a small overhead over vanilla IBP, and the cost is still lower than that of CROWN-IBP. Meanwhile, our method is able to achieve lower verified errors compared to the two baselines (Table 1 and Table 2). More importantly, we are able to use much shorter training schedules to achieve SOTA results compared to previous literature, which enables faster certified robust training.

B.2 Additional Ablation Study

In this section, we present additional ablation study results on BN, where we split the centralization (the shifting operation using the mean) and the unitization (the scaling operation using the variance)

Table 7: Comparison of estimated time cost (seconds) on all the datasets and models. We report the per-epoch time during training phases with different ϵ ranges, and we report the total time when the 70-epoch schedule is used for MNIST, the 160-epoch schedule for CIFAR-10, and the 80-epoch schedule for TinyImageNet respectively. “-” in the table means that there is no $\epsilon = 0$ warmup stage for MNIST following Zhang et al. (2020). Note that on each dataset, for phases of same or different methods that are supposed to be equivalent in algorithm implementation, we make them share the same time estimation result respectively.

Dataset	Model	Method	Per-epoch for ϵ			Total
			0	$(0, \epsilon_{\text{target}})$	ϵ_{target}	
MNIST	CNN-7	Vanilla IBP	-	27.9	27.9	1955.1
		CROWN-IBP	-	49.6	27.9	2387.5
		Ours	-	37.0	27.9	2135.8
	Wide-ResNet	Vanilla IBP	-	81.0	81.0	5668.3
		CROWN-IBP	-	142.1	81.0	6890.2
		Ours	-	99.0	81.0	6029.3
	ResNeXt	Vanilla IBP	-	73.2	73.2	5127.2
		CROWN-IBP	-	147.7	73.2	6616.9
		Ours	-	104.4	73.2	5750.7
CIFAR-10	CNN-7	Vanilla IBP	30.0	54.8	54.8	8747.9
		CROWN-IBP	30.0	78.5	54.8	10641.3
		Ours	64.0	64.0	54.8	9512.3
	Wide-ResNet	Vanilla IBP	43.7	114.7	114.7	18358.4
		CROWN-IBP	43.7	170.7	114.7	22764.9
		Ours	134.7	134.7	114.7	19976.0
	ResNeXt	Vanilla IBP	38.7	102.7	102.7	16432.0
		CROWN-IBP	38.7	183.3	102.7	22813.6
		Ours	129.6	129.6	102.7	18611.7
TinyImageNet	CNN-7	Vanilla IBP	282.2	431.4	431.4	34362.0
		CROWN-IBP	282.2	663.8	431.4	36686.5
		Ours	500.4	500.4	431.4	35270.3
	Wide-ResNet	Vanilla IBP	270.2	399.8	399.8	31861.6
		CROWN-IBP	270.2	592.1	399.8	33789.3
		Ours	464.6	464.6	399.8	32703.0
	ResNeXt	Vanilla IBP	197.2	430.5	430.5	34206.7
		CROWN-IBP	197.2	883.1	430.5	38735.1
		Ours	626.3	626.3	430.5	36595.8

Table 8: Additional ablation study results on BN where we consider whether centralization and unitization in BN present respectively. The results are from CNN-7 on CIFAR-10 ($\epsilon_{\text{target}} = 8/255$) using the training schedule with 160 epochs in total. We compare the proportion of active ReLU neurons and inactive ReLU neurons respectively, and also the errors.

Centralization	Unitization	Active ReLU (%)	Inactive ReLU (%)	Standard error (%)	Verified error (%)
×	×	7.37±0.25	90.57±0.30	57.36±0.45	69.91±0.31
✓	×	13.48±0.22	84.73±0.26	55.36±0.17	68.07±0.02
×	✓	16.94±0.79	80.40±0.75	54.41±0.49	67.78±0.46
✓	✓	21.30±0.39	75.90±0.40	51.72±0.40	65.58±0.30

to investigate whether both of them contribute to the improvement by BN. We run this experiment for CNN-7 on CIFAR-10 ($\epsilon_{\text{target}} = 8/255$) using the training schedule with 160 epochs in total, and we show the results in Table 8.

From our ablation results, we can observe that both centralization and unitization in BN contribute to the improvement. We conclude the benefit as follows. First, BN has inherent benefits for standard DNN training (Ioffe & Szegedy, 2015; Van Laarhoven, 2017; Santurkar et al., 2018). In addition, BN benefits IBP also because it has an effect on balancing ReLU neuron states, as our results show that when a model is trained with BN, the number of active ReLU neurons is noticeably better than the cases without BN. We found that actually both mean centralization and unitization help to balance active and inactive ReLU neurons. It is easy to understand that centralization helps balancing as it can center the bounds around zero. For unitization, we conjecture that it helps the optimization for DNN (from the acceleration or smoothing the loss landscape perspective for standard DNN training),

and this may allow the model to have a less tendency to reduce the robust loss by trivially making most neurons inactive.

B.3 Other Perturbation Radii

In Table 9, we present results using perturbation radii other than those used in our main experiments. Here we consider $\epsilon_{\text{target}} \in \{0.1, 0.3\}$ for MNIST, and $\epsilon_{\text{target}} \in \{\frac{2}{255}, \frac{16}{255}\}$ for CIFAR-10. In particular, on MNIST models are trained with target perturbation radii ϵ_{train} larger than used for testing ϵ_{target} to mitigate overfitting – we use $\epsilon_{\text{train}} = 0.2$ when $\epsilon_{\text{target}} = 0.1$ and $\epsilon_{\text{train}} = 0.4$ when $\epsilon_{\text{target}} = 0.3$ following Zhang et al. (2020). We use CNN-7 in this experiment. Results show that improvements over Vanilla IBP and CROWN-IBP are consistent as in Table 1. Note that CIFAR-10 with very small $\epsilon = \frac{2}{255}$ is a special case where using pure linear relaxation bounds (Wong & Kolter, 2018; Zhang et al., 2020) for training yields even lower errors than IBP (Gowal et al., 2018) and standard CROWN-IBP which anneals to IBP training after warmup. On this setting, an alternative version of CROWN-IBP that does not anneal to IBP training can achieve lower verified error 43.61% without loss fusion (60.44% if loss fusion is enabled). However, using pure linear relaxation bounds for certified training is more costly and usually has worse results on other settings (Jovanović et al., 2021). Thus for all the other settings in Zhang et al. (2020), CROWN-IBP still have to anneal to IBP training, as the version we adopt in our main experiments. Overall, the experimental results demonstrate that our proposed method is effective on settings with different perturbation radii, compared to vanilla IBP and CROWN-IBP.

Table 9: The standard errors (%) and verified errors (%) of a CNN-7 model trained with different methods on other perturbation radii not included in the main results.

Dataset	Warmup	ϵ_{target}	ϵ_{train}	Vanilla IBP		CROWN-IBP		Ours	
				Standard	Verified	Standard	Verified	Standard	Verified
MNIST	0+20	0.1	0.2	1.12	2.17	1.07	2.17	1.16	2.05
		0.3	0.4	2.74	7.61	2.88	7.55	2.33	6.90
CIFAR-10	1+80	2/255		33.65	48.75	34.09	48.28	33.16	47.15
		16/255		64.52	76.36	71.75	79.43	63.35	75.52

B.4 Sensitivity on the λ_0 Hyperparameter

To test the sensitivity of the training performance on the choice of λ_0 , we run an experiment on CNN-7 for CIFAR-10 ($\epsilon_{\text{target}} = 8/255$) using the 160-epoch schedule. We consider $\lambda_0 \in \{0.1, 0.2, 0.5, 1.0, 2.0\}$, and we run 5 repeated experiments for each setting to report the mean and standard deviation. We show the results in Table 10.

We find that $\lambda_0 = 0.5$ or $\lambda_0 = 1.0$ both yield good results on this setting. Actually, for all the results of “ours” in Table 1 (MNIST and CIFAR-10) in the paper, we always use $\lambda_0 = 0.5$ for all settings, and we do not tune λ_0 for each setting individually. This suggests that potential users do not need to search for λ_0 in each training. Similarly, on TinyImageNet, good results can be achieved by using $\lambda_0 = 0.1$ for all the settings. The λ_0 for TinyImageNet is smaller, and this can be explained by smaller ϵ_{target} for TinyImageNet ($1/255$) compared to 0.4 for MNIST and $8/255$ for CIFAR-10. Thus, the results suggest that our approach is not very sensitive to choice of λ_0 , and a reasonable default value can work well for many settings (e.g., under many different training schedules or models).

Table 10: Results of the sensitivity test for the λ_0 hyperparameter, on CNN-7 for CIFAR-10 ($\epsilon_{\text{target}} = 8/255$) using the 160-epoch schedule.

λ_0	0.1	0.2	0.5	1.0	2.0
Standard error (%)	53.03 ± 0.56	53.08 ± 0.62	51.72 ± 0.40	50.98 ± 0.33	53.80 ± 0.37
Verified error (%)	66.44 ± 0.24	66.54 ± 0.48	65.58 ± 0.32	65.42 ± 0.22	66.91 ± 0.26

B.5 Applying the Proposed Method to CROWN-IBP

We have tried applying our method to CROWN-IBP (Zhang et al., 2020) besides IBP. On CNN-7 for CIFAR-10 ($\epsilon_{\text{target}} = 8/255$) with the 160-epoch training schedule, we observe that adding BN improves the performance of CROWN-IBP (verified error 68.02% \rightarrow 66.93% if loss fusion is disabled; 76.11% \rightarrow 68.8% if loss fusion is enabled). However, further adding IBP initialization or the warmup regularizers does not significantly change the performance. For the possible reasons of this result, we analyze that: 1) CROWN-IBP already has tighter bounds by a linear relaxation based bound propagation; 2) CROWN-IBP has tight relaxation for both inactive and active ReLU neurons, compared to IBP which has tight relaxation only for inactive neurons but not active ones, so the imbalanced ReLU issue is less significant for CROWN-IBP (For the setting in Figure 2, we empirically find that even if we do not use warmup regularization, CROWN-IBP already has around 19% active neurons, even more than our improved IBP). Thus, it is reasonable that our proposed method focusing on improving bound tightness and ReLU neuron balance may be less effective for CROWN-IBP.

Instead, there may be other factors that limit the performance of linear relaxation based certified robust training. So far tighter linear or convex relaxation bounds (e.g., Zhang et al. (2018) or Wong & Kolter (2018)) usually cannot outperform pure IBP using looser interval bounds. While Zhang et al. (2020) used linear relaxation bounds for certified training and outperformed pure IBP, their method still needs to gradually anneal to pure IBP bounds in the end of training. There are some recent works that studied the reasons behind this phenomenon. Jovanović et al. (2021) identified two properties of convex relaxations, continuity and sensitivity, that may impact training dynamics. Lee et al. (2021) identified a factor about the smoothness of loss landscape, and they proposed to use tighter relaxation via optimizing the bounds, which may lead to more favorable loss landscapes. In terms of improving the verified errors after training, Jovanović et al. (2021) only have preliminary results on a small network for MNIST since their new relaxations require solving convex/linear programs; and we outperform Lee et al. (2021) (15.42% for MNIST $\epsilon_{\text{target}} = 0.4$; 69.70% for CIFAR-10 $\epsilon_{\text{target}} = 8/255$) with a notable margin, while we use much shorter training schedules.

B.6 Comparison with Randomized Smoothing

In this section, we empirically compare the performance of our method with randomized smoothing methods. As we have mentioned in Sec. 2, randomized smoothing is mostly suitable for ℓ_2 -norm certified defense, and it is fundamentally limited for ℓ_∞ norm robustness. But there are still existing works such as Salman et al. (2019) that use norm inequalities to convert ℓ_2 norm robustness certificates to an ℓ_∞ norm one. For ℓ_∞ -norm perturbation radius $\epsilon = \frac{8}{255}$ on CIFAR-10 where each input image has $3 \times 32 \times 32$ dimensions, we can convert it to ℓ_2 -norm radius $\epsilon_2 = \frac{8}{255} \times \sqrt{3 \times 32 \times 32} = 1.73884$ used by randomized smoothing such that the certified accuracy under this ℓ_2 perturbation provides a lower bound for ℓ_∞ certified robustness under radius $\epsilon = \frac{8}{255}$. In an earlier work (Li et al., 2019), their certified accuracy under this perturbation size is 0, according to their Figure 1; and in a more recent work (Salman et al., 2019), according to results in their Table 7, their best certified accuracy is 23% for radius 1.75, and the certified accuracy is 26% for radius 1.5, so their certified error is at least 74% for $\ell_\infty \epsilon = 8/255$. Therefore, the certified error we achieve in our paper is much lower (65.58 \pm 0.32%), compared to randomized smoothing by converting ℓ_2 certified radius.

B.7 ReLU Imbalance with Shorter Warmup Length

In Figure 2, we show two 7-layer CNN models with different warmup length respectively, and the model tends to have more inactive neurons and thus more severe imbalance in ReLU neuron states for shorter warmup length, as previously mentioned in Section 3.2.2.

B.8 Using IBP Initialization when Bound Explosion is More Severe

In Figure 7, we show that for a ResNeXt on TinyImageNet, where the explosion of certified bounds is more severe if the network is initialized with standard weight initialization, using our proposed initialization is helpful for reaching lower verified errors especially at early epochs.

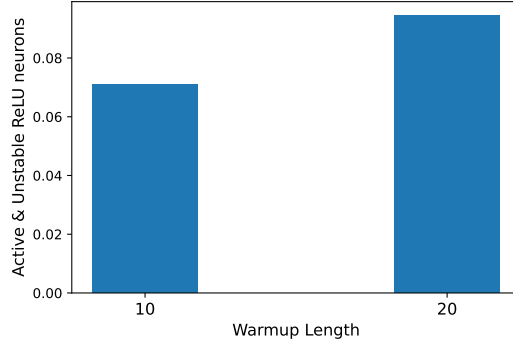


Figure 6: Ratio of active and unstable neurons in CNN-7 trained with Vanilla IBP using different warmup lengths respectively.

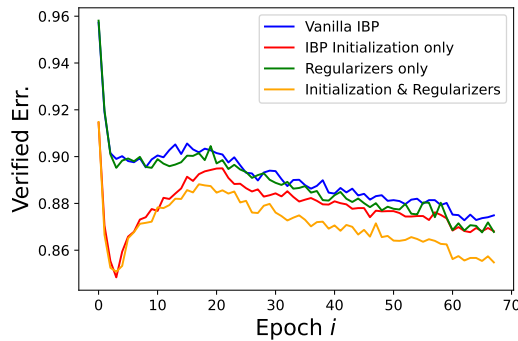


Figure 7: Curve of training verified error of a ResNeXt model on TinyImageNet. Note that the verified errors can increase during the warmup as ϵ increases.

C Experimental Details

Implementation Our implementation is based on the `auto_LiRPA` library (Xu et al., 2020)¹ which supports robustness verification and training on general computational graphs. Baselines including Vanilla IBP and CROWN-IBP with loss fusion are inherently supported by the library. We add to implement our IBP initialization and warmup with regularizers for fast certified robust training.

Datasets For MNIST and CIFAR-10, we load the datasets using `torchvision.datasets`² and use the original data splits. On CIFAR-10, we use random horizontal flips and random cropping for data augmentation, and also normalize input images, following Zhang et al. (2020); Xu et al. (2020). For TinyImageNet, we download the dataset from Stanford CS231n course website³. Similar to CIFAR-10, we also use data augmentation and normalize input images for TinyImageNet. Unlike Xu et al. (2020) which cropped the 64×64 original images into 56×56 and used a central 56×56 cropping for test images, we pad the cropped training images back to 64×64 so that we do not need to crop test images. We use the validation set for testing since test images are unlabelled, following Xu et al. (2020).

Models We use three model architectures in the experiments: a 7-layer feedforward convolutional network (CNN-7), Wide-ResNet (Zagoruyko & Komodakis, 2016) and ResNeXt (Xie et al., 2017). All the models have a hidden fully-connected layer with 512 neurons prior to the classification layer. For CNN-7, there are five convolutional layers with 64, 64, 128, 128, 128 filters respectively. For Wide-ResNet, there are 3 wide basic blocks, with a widen factor of 8 for MNIST and CIFAR-10 and 10 for TinyImageNet. For ResNeXt, we use 1, 1, 1 blocks for MNIST and CIFAR-10, and 2, 2, 2

¹https://github.com/KaidiXu/auto_LiRPA

²<https://pytorch.org/vision/0.8/datasets.html>

³<http://cs231n.stanford.edu/TinyImageNet-200.zip>

blocks for TinyImageNet; the cardinality is set to 2, and the bottleneck width is set to 32 for MNIST and CIFAR-10 and 8 for TinyImageNet. For all the models, ReLU is used as the activation. These models were similarly adopted in Xu et al. (2020). But we fully add BNs after each convolutional layer and fully-connected layer, while some of these BNs were missed in Xu et al. (2020). For example, the CNN-7 model in Xu et al. (2020) had BN for convolutional layers but not the fully-connected layer. Besides, we remove the average pooling layer in Wide-ResNet as we find it harms the performance of all the considered training methods, and this modification makes the Wide-ResNet align better with the CNN-7 model, which does not have average pooling either and achieves best results compared to other models (Table 1 and Table 2).

Training During certified training, models are trained with Adam (Kingma & Ba, 2014) optimizer with an initial learning rate of 5×10^{-4} , and there are two milestones where the learning rate decays by 0.2. We determine the milestones for learning rate decay according to the training schedule and the total number of epochs, as shown in Table 11. Gradient clipping threshold is set to 10.0. We train the models using a batch size of 256 on MNIST, and 128 on CIFAR-10 and TinyImageNet. The tolerance value τ in our warmup regularization is fixed to 0.5. For Vanilla IBP and IBP with our initialization and regularizers, we train the models on a single NVIDIA GeForce GTX 1080 Ti or NVIDIA GeForce RTX 2080 Ti GPU for each setting. For CROWN-IBP, we train the models on two GPUs for efficiency, while in time estimation we still use one single GPU for fair comparison. The number of training and evaluation runs is 1 for each experiment result respectively. In the evaluation, the major metric is *verified error*, which stands for the rate of test examples such that the model cannot certifiably make correct predictions given the ℓ_∞ perturbation radius. For reference, we also report *standard error*, which is the standard error rate where no perturbation is considered.

Table 11: Milestones for learning rate decay when different total number of epochs are used. ‘‘Decay-1’’ and ‘‘Decay-2’’ denote the two milestones respectively when the learning rate decays by a factor of 0.2.

Dataset	Total epochs	Decay-1	Decay-2
MNIST	50	40	45
	70	50	60
CIFAR-10	70	50	60
	160	120	140
TinyImageNet	80	60	70

Warmup scheduling During the warmup stage, after training with $\epsilon = 0$ for a number of epochs, the perturbation radius ϵ is gradually increased from 0 until the target perturbation radius ϵ_{target} , during the $0 < \epsilon < \epsilon_{\text{target}}$ phase. Specifically, during the first 25% epochs of the ϵ increasing stage, ϵ is increased exponentially, and after that ϵ is increased linearly. In this way, ϵ remains relatively small and increases relatively slowly during the beginning, to stabilize training. We use the `SmoothedScheduler` in the `auto_LiRPA` as the scheduler for ϵ similarly adopted by Xu et al. (2020). On CIFAR-10, unlike some prior works which made the perturbation radii used for training 1.1 times of those for testing respectively (Gowal et al., 2018; Zhang et al., 2020), we find this setting makes little improvement over using same perturbation radii for both training and testing in our experiments as also mentioned in Lee et al. (2021), and thus we directly adopt the later setting for simplicity.

D Mathematical Proofs

D.1 Proof of Eq. (5)

In this section, we provide a proof for Eq. (5):

$$\mathbb{E}(\delta_i) = \mathbb{E}(\text{ReLU}(\bar{\mathbf{h}}_i) - \text{ReLU}(\underline{\mathbf{h}}_i)) = \frac{1}{2}\mathbb{E}(\Delta_i), \quad (11)$$

where $\Delta_i = \bar{\mathbf{h}}_i - \underline{\mathbf{h}}_i$, and $\delta_i = \bar{\mathbf{z}}_i - \underline{\mathbf{z}}_i$.

Proof. We first have

$$\begin{aligned}
\mathbb{E}(\delta_i) &= \mathbb{E}(\text{ReLU}(\bar{\mathbf{h}}_i) - \text{ReLU}(\underline{\mathbf{h}}_i)) \\
&= \mathbb{E}(\text{ReLU}(\mathbf{c}_i + \frac{\Delta_i}{2}) - \text{ReLU}(\mathbf{c}_i - \frac{\Delta_i}{2})) \\
&= \mathbb{E}(\text{ReLU}(\mathbf{c}_i + \frac{\Delta_i}{2})) - \mathbb{E}(\text{ReLU}(\mathbf{c}_i - \frac{\Delta_i}{2})).
\end{aligned} \tag{12}$$

Note that $\mathbf{c}_i = \frac{1}{2}\mathbf{W}_i(\underline{\mathbf{z}}_i + \bar{\mathbf{z}}_i)$ and $\Delta_i = |\mathbf{W}_i|\delta_i$, and thus $p(-\mathbf{c}_i | |\mathbf{W}_i|) = p(\mathbf{c}_i | |\mathbf{W}_i|)$ and $p(-\mathbf{c}_i|\Delta_i) = p(\mathbf{c}_i|\Delta_i)$, where we use $p(\cdot)$ to denote the probability density function (PDF). Thereby,

$$\begin{aligned}
\mathbb{E}(\text{ReLU}(\mathbf{c}_i + \frac{\Delta_i}{2})) &= \int_0^\infty \int_{-\frac{\Delta_i}{2}}^\infty (\mathbf{c}_i + \frac{\Delta_i}{2}) p(\mathbf{c}_i|\Delta_i) p(\Delta_i) d\mathbf{c}_i d\Delta_i, \\
\mathbb{E}(\text{ReLU}(\mathbf{c}_i - \frac{\Delta_i}{2})) &= \int_0^\infty \int_{\frac{\Delta_i}{2}}^\infty (\mathbf{c}_i - \frac{\Delta_i}{2}) p(\mathbf{c}_i|\Delta_i) p(\Delta_i) d\mathbf{c}_i d\Delta_i.
\end{aligned} \tag{13}$$

And thus

$$\begin{aligned}
&\mathbb{E}(\text{ReLU}(\mathbf{c}_i + \frac{\Delta_i}{2})) - \mathbb{E}(\text{ReLU}(\mathbf{c}_i - \frac{\Delta_i}{2})) \\
&= \int_0^\infty \left(\int_{\frac{\Delta_i}{2}}^\infty \Delta_i + \int_{-\frac{\Delta_i}{2}}^{\frac{\Delta_i}{2}} (\mathbf{c}_i + \frac{\Delta_i}{2}) \right) p(\mathbf{c}_i|\Delta_i) p(\Delta_i) d\mathbf{c}_i d\Delta_i \\
&= \int_0^\infty \int_{-\infty}^\infty \frac{\Delta_i}{2} p(\mathbf{c}_i|\Delta_i) p(\Delta_i) d\mathbf{c}_i d\Delta_i \\
&= \frac{1}{2} \mathbb{E}(\Delta_i).
\end{aligned} \tag{14}$$

□

D.2 Proof on the Bounds of $\text{Var}(\underline{\mathbf{h}}_i)$ and $\text{Var}(\bar{\mathbf{h}}_i)$

In this section, we show that $\text{Var}(\underline{\mathbf{h}}_i)$ and $\text{Var}(\bar{\mathbf{h}}_i)$ will not explode or vanish at initialization, so that the magnitude of forward signals will not vanish or explode when we use IBP initialization which focuses on stabilizing the tightness of certified bounds.

We can derive that

$$\begin{aligned}
\text{Var}(\bar{\mathbf{h}}_i) &= \text{Var}(\mathbf{W}_{i,+}\bar{\mathbf{z}}_{i-1} + \mathbf{W}_{i,-}\underline{\mathbf{z}}_{i-1}) \\
&= \text{Var}([\mathbf{W}_{i,+}\bar{\mathbf{z}}_{i-1} + \mathbf{W}_{i,-}\underline{\mathbf{z}}_{i-1}]_j) \quad (0 \leq j \leq r_i) \\
&= \text{Var}\left(\sum_{k=1}^{n_i} ([\mathbf{W}_i]_{j,k} [\bar{\mathbf{z}}_{i-1}]_k \cdot \mathbb{I}([\mathbf{W}_i]_{j,k} > 0)) \right. \\
&\quad \left. + \sum_{k=1}^{n_i} ([\mathbf{W}_i]_{j,k} [\underline{\mathbf{z}}_{i-1}]_k \cdot \mathbb{I}([\mathbf{W}_i]_{j,k} \leq 0))\right).
\end{aligned}$$

Since \mathbf{W}_i is initialized with mean 0, the numbers of negative elements and positive elements are approximately equal, and thus

$$\begin{aligned}
\text{Var}(\bar{\mathbf{h}}_i) &\approx \frac{n_i}{2} \text{Var}(\mathbf{W}_{i,+}\bar{\mathbf{z}}_{i-1}) + \frac{n_i}{2} \text{Var}(\mathbf{W}_{i,-}\underline{\mathbf{z}}_{i-1}) \\
&= \frac{n_i}{2} \left(\text{Var}(\mathbf{W}_{i,+}) \mathbb{E}(\bar{\mathbf{z}}_{i-1})^2 \right. \\
&\quad \left. + \text{Var}(\bar{\mathbf{z}}_{i-1}) \mathbb{E}(\mathbf{W}_{i,+})^2 + \text{Var}(\mathbf{W}_{i,-}) \mathbb{E}(\underline{\mathbf{z}}_{i-1})^2 + \text{Var}(\underline{\mathbf{z}}_{i-1}) \mathbb{E}(\mathbf{W}_{i,-})^2 \right) \\
&= \frac{\pi}{n_i} \left(1 - \frac{2}{\pi}\right) \mathbb{E}(\bar{\mathbf{z}}_{i-1}^2) + \frac{2}{n_i} \text{Var}(\bar{\mathbf{z}}_{i-1}) + \frac{\pi}{n_i} \left(1 - \frac{2}{\pi}\right) \mathbb{E}(\underline{\mathbf{z}}_{i-1}^2) + \frac{2}{n_i} \text{Var}(\underline{\mathbf{z}}_{i-1}).
\end{aligned}$$

Note that $\mathbb{E}(\bar{\mathbf{z}}_i) \geq \mathbb{E}(\delta_i)$ and we have made $\mathbb{E}(\delta_i)$ stable in each layer. Thus $\text{Var}(\bar{\mathbf{h}}_i) \geq \frac{n_i}{2} \text{Var}(\mathbf{W}_{i,+}) \mathbb{E}(\bar{\mathbf{z}}_{i-1})^2$ and will not vanish when the network goes deeper. Also note that $n_i > 1$ in neural networks, and therefore $\text{Var}(\bar{\mathbf{h}}_i)$ will not explode. The same analysis can also be applied to $\underline{\mathbf{h}}_i$.

However, when we use the IBP initialization, variance of the standard forward value \mathbf{h}_i will be smaller than that of Xavier and Kaiming Initialization. Following the analysis in He et al. (2015a), we have

$$\text{Var}(\mathbf{h}_i) = \frac{n_i}{2} \text{Var}(\mathbf{W}_i) \text{Var}(\mathbf{h}_{i-1}).$$

In IBP initialization, we have $\text{Var}(\mathbf{W}_i) = \frac{2\pi}{n_i}$, and the variance of \mathbf{h}_i can become smaller after going through each affine layer. Therefore, as mentioned in Section 4.4, simply adding IBP initialization may not finally improve the verified error, because it may harm the early warmup when ϵ is small and certified training is close to standard training. In this paper, in addition to IBP initialization, we further add regularizers to stabilize certified bounds and the balance of ReLU neuron states, while the variance is stabilized by fully adding BN. The effect of these parts of our proposed method is discussed in Section 4.4.